Proceedings of the 3rd International Conference on Expansive Soils, Jerusalem Academic Press, Israel Institute of Technology, Technion City, pp. 97-108. Haifa, Israel. 1973

PRESSURE RESPONSE BELOW HIGH AIR ENTRY DISCS

INTRODUCTION

Numerous research workers have attempted to incorporate the flexibility of the measuring system (compliance) into the analysis of pore pressure measurements. The research has been directed mainly toward the analysis of pore pressure measurements at the base of a sample in a one-dimensional oedometer.

Whitman, Richardson and Healy (1961) used an electrical analog to simulate the flexibility of pore pressure measuring systems. Gibson (1963) theoretically examined the time lag in an open and closed pore pressure measuring system at the base of a clay layer. The time lag has been attributed to the permeability of the soil, k, the compressibility of the soil, m_v, and the flexibility of the measuring system, λ. These factors are combined to form the stiffness ratio, η.

$$\eta = \frac{A \cdot k \cdot H}{\gamma_w \cdot c_v \cdot \lambda} = \frac{A \cdot H \cdot m_v}{\lambda} \qquad \ldots 1)$$

where A = cross-sectional area of the sample

H = height of the sample

c_v = coefficient of consolidation

γ_w = density of water

Perloff, Nair and Smith (1965), Northey and Thomas (1965) and Christie (1965) used the above definition of stiffness ratio and expanded the analytical solution to describe the distribution of pore pressure throughout a sample during one-dimensional consolidation. Attempts to correlate the theory with laboratory tests have met with limited success.

The above studies assumed that the flexibility of the measuring system involved:

i) a linear compressible fluid in the measuring system

ii) a linear expansibility of the pipes, valves and transducer diaphragm.

Whitman et al (1961) reported that "even a modest amount of air in the measuring system will not introduce great error". Christie (1965) states that entrapped air "has the effect of increasing the flexibility of the measuring system by an unknown amount".

This paper discusses the factors associated with the pore pressure measuring system that effect the pressure response.

PRESSURE RESPONSE THEORY

The model used to characterize the reaction of the pressure transducer is shown in Figure 1. Initially one valve on the base plate is left open and water seeps from the chamber through the high air entry disc under steady state conditions. When the valve is closed, the flow of water into the base plate causes a compression of the fluid resulting in a build-up of pressure (as

measured on the transducer). The increase in compartment pressure reduces the hydraulic gradient across the disc and lessens the inflow of water. Equilibrium is reached when the pressure in the base plate is equal to the pressure applied to the water in the chamber.

There are two possible sources of volume change; namely, the base plate compartment and the air-water mixture in the compartment. The first factor depends on the rigidity of the base plate construction, thickness and method of mounting the ceramic disc, the deflection of the transducer membrane and volume change in the two base plate valves during the pressure build-up. All these factors tend to produce a final compartment in the base plate that is larger under pressure than its initial size.

Flow across the high air entry disc occurs in accordance with Darcy's law. The gradient is continuously changing and can be written in finite difference form.

$$\Delta Q = k_d \cdot i_{ave} \cdot A_d \cdot (t_j - t_i) \qquad \ldots 2)$$

where ΔQ = flow during a time increment

k_d = coefficient of permeability of the ceramic disc

i_{ave} = average hydraulic gradient for the time increment

A_d = cross-sectional area of ceramic disc

t_j = end of time increment

t_i = start of time increment

An average hydraulic gradient is assumed to apply for the present time increment. The hydraulic gradient is then recomputed for the next time period. The gradient during the period t_i to t_j is,

$$i_{ave} = \frac{1}{\gamma_w} \cdot \left[\frac{\frac{(u_c - u_i)}{d} + \frac{(u_c - u_j)}{d}}{2} \right] \quad \ldots 3)$$

where u_c = pressure applied to the water in the chamber

u_i = compartment pressure at time, t_i

u_j = compartment pressure at time, t_j

d = thickness of the high air entry disc

Substituting into Darcy's flow equation gives:

$$\Delta Q = \frac{k_d \cdot A_d}{\gamma_w \cdot d} \cdot \left[u_c - \frac{(u_i + u_j)}{2} \right] \cdot (t_j - t_i) \quad \ldots 4)$$

The quantity of flow, ΔQ, must equal the compression of the air-water mixture in the compartment, ΔV_m, plus the expansion of the compartment, ΔV_c.

$$\Delta Q = \Delta V_c + \Delta V_m \quad \ldots 5)$$

The expansion of the compartment can be represented as:

$$\Delta V_c = \beta_c \cdot (u_j - u_i) \cdot V \quad \ldots 6)$$

where β_c = composite compressibility of the materials composing the compartment

V = volume of the compartment

Initially, let us assume this value is negligible in comparison to the volume change associated with the compression of the air-water mixture in the compartment.

$$\Delta V_m = \beta_m \cdot V \cdot (u_j - u_i) \qquad \ldots 7)$$

Substituting into equation 4) gives:

$$\beta_m = \frac{k_d \cdot A_d}{d \cdot V \cdot \gamma_w} \cdot \left[\frac{u_c - \frac{(u_i + u_j)}{2}}{(u_j - u_i)} \right] \cdot (t_j - t_i) \qquad \ldots 8)$$

Let the compliance factor of the measuring system be defined as,

$$C = \frac{\gamma_w \cdot V \cdot d}{k_d \cdot A_d} \qquad \ldots 9)$$

In the laboratory, it is possible to measure the pressure response by means of a high-speed data acquisition system. By marching forward in time and substituting the measured pressures into equation 8) it is possible to compute the compressibility of the mixture in the compartment.

THEORETICAL RESPONSE RELATIONSHIPS

To develop theoretical response curves, it is necessary to have a constitutive equation for the fluid in the compartment. Let us assume that the compartment contains a mixture of air and water, and that with time, de-aired water flows through the high air entry disc, compressing the mixture. Therefore, the compressibility is continuous changing but can be written in terms of the pressure and the initial percentage of air in the compartment. It is also assumed that no further air comes out of solution in the compartment and that the time involved is insufficient for the dissolving of free air. Computations based on a diffusivity of 2×10^{-5} cm^2/sec show that the above assumption is certainly reasonable for elapsed times less than 10 minutes.

The compressibility for an immiscible air-water mixture, β_m, can be defined as,

$$\beta_m = \frac{-1}{V} \cdot \left[\frac{dV_w}{du_w} + \frac{dV_a}{du_a} \right] \qquad \ldots 10)$$

where V = volume of the compartment

V_w = volume of water in the compartment

V_a = volume of air in the compartment

u_w = pressure in the water phase

u_a = pressure in the air phase

For the water phase,

$$\frac{dV_w}{du_w} = -\beta_w \cdot V_w \qquad \ldots 11)$$

and for the air phase,

$$\frac{dV_a}{du_a} = - \frac{V_{ao} \cdot u_{ao}}{u_a^2} \qquad \ldots 12)$$

where β_w = compressibility of de-aired water

V_{ao} = initial volume of air in the compartment

u_{ao} = initial air pressure

Writing the volumes in terms of the initial degree of saturation, S_o, and assuming that the air and water pressures are equal, gives the following equation for the compressibility of the mixture.

$$\beta_m = \beta_w \cdot S_o + \frac{(1 - S_o)\, u_{ao}}{u_a^2} \qquad \ldots 13)$$

The validity of the compressibility equation was examined by altering the pressure in the compartment and accurately monitoring the volume change (Figure 2). No water escaped through the high air entry disc since the air pressure in the chamber was always higher than the compartment pressure. A slotted aluminum block was placed over the high air entry disc and subjected to a high total pressure to prevent deflections. The volume of water entering the compartment was converted to a compressibility and plotted versus the chamber pressure (Figure 3). The results of the two tests indicate close agreement between the theoretical and measured constitutive relationship for the air-water mixture.

Starting with an assumed percentage of air in the compartment, the response time for a chosen pressure increase can be evaluated by combining equations 8) and 13).

$$t_j - t_i = \frac{\beta_m \cdot C \cdot (u_j - u_i)}{\left[u_c - \frac{(u_i + u_j)}{2}\right]} \qquad \ldots 14)$$

Subsequent response time intervals are computed by incrementing the compartment pressure. The summation of the response time intervals gives the time corresponding to each measured pressure.

The development of pressure response can also be written as a continuous function. The time increment is written as,

$$dt = C \cdot \beta_w \cdot S_o \cdot \frac{du}{(u_c - u)} + C \cdot u_{ao} (1 - S_o) \cdot \frac{du}{u^2(u_c - u)} \qquad \ldots 15)$$

where u = the compartment pressure at any time.

Equation 15) must be integrated to obtain an equation which allows the computation of the elapsed time corresponding to any pore pressure response.

$$t = -K_1 \log (u_c - u) - K_2 \cdot \left[\frac{1}{u_c \cdot u} + \frac{1}{u_c^2} \cdot \log\left(\frac{u_c - u}{u}\right)\right] + K_3 \qquad \ldots 16)$$

where $K_1 = C \cdot \beta_w \cdot S_o$ and

$$K_2 = C \cdot u_{ao} \cdot (1 - S_o)$$

Using the initial boundary conditions stating that the initial mixture pressure is equal to atmospheric pressure, the constant, K_3, is computed.

$$K_3 = K_1 \log (u_c - u_{ao}) + K_2 \cdot \left[\frac{1}{u_c \cdot u_{ao}} + \frac{1}{u_c^2} \log \left(\frac{u_a - u_{ao}}{u_{ao}} \right) \right] \quad \ldots 17)$$

Substituting equation 17) into equation 16) gives,

$$t = k_1 \log \left(\frac{u_c - u_{ao}}{u_c - u} \right) + K_2 \cdot \frac{1}{u_c^2} \cdot \log \left(\frac{u_c - u_{ao}}{u_c - u} \cdot \frac{u}{u_{ao}} \right) +$$

$$K_2 \cdot \left[\frac{1}{u_c} \cdot \left(\frac{1}{u_{ao}} - \frac{1}{u} \right) \right]$$

Figure 4 shows typical response curves for compliance factors ranging from 100 to 100,000 and an initial air content of two percent. The wide range of compliance factors corresponds to the variation in coefficient of permeability associated with the high air entry ceramic discs. A changing of the compliance factor merely shifts the response curves laterally.

Changing the initial air content while keeping the compliance factor constant, also causes a lateral shift in the response curves (Figure 5). The slope of the steepest portion of the

response curves remains essentially constant as long as the initial air content is greater than approximately one percent.

The effect of changing the applied chamber pressure is examined for a compliance factor of 10,000 and an initial air content of two percent (Figure 6). The slope of the steepest portion of the response curve decreases and the time required for pressure equalization increases as the applied chamber pressure decreases.

The theoretical response curves show that only two variables are required to describe them:

i) The slope of the straight line portion of the response curve on a semi-logarithm plot, and

ii) One point representing the lateral shift of the response curve. Any point between 40 and 80 percent response could be used for correlation purposes; however, a more meaningful value is obtained using the point of intersection of the extended straight line portion of the response curve and the horizontal line of 100 percent response. This point is termed the "equalization time".

The "equalization time" depends on:

i) the initial air content,

ii) the compliance factor of the system, and

iii) the applied chamber pressure.

Figure 7 shows a plot of the logarithm of equalization time versus logarithm of compliance factor for an applied chamber pressure of 100 psi. Lines of equal initial air content are linear on this plot and are spaced at a constant logarithmic

scale except at the low air content range.

PRESENTATION AND DISCUSSION OF PRESSURE RESPONSE DATA

Approximately 24 pressure response tests were performed with a range of:

i) ceramic disc thicknesses,

ii) air entry and permeability values,

iii) applied chamber pressures and

iv) initial percentages of air.

In order to compute the compliance factor of the measuring system it is necessary to measure the volume of the compartment. Estimates of volume were obtained by saturating the compartment with water, opening the valves and blowing out the water into a beaker (Table I).

TABLE I

Volume of Compartment in Measuring Systems

Apparatus No.	Volume (cc)
Triaxial #2	6.79
Anteus Oedometer #177	4.20
Anteus Oedometer #179	3.90

Table II chronologically summarizes the details of the response tests. Typical pressure response with time curves and the compressibility versus pressure curves are presented in Figures 8 and 9 respectively. The pressure response curves show

TABLE II

SUMMARY OF RESPONSE TESTS ON CERAMIC DISCS

Apparatus No.	Date	Air Entry Value (Bars)	Thickness (cm)	Permeability (cm/sec)	Applied Pressure (psi)	Equalization Time (min)	Final Vol. of Air (cc)
Oed. #179	Oct. 27/71	15	0.306	8.41×10^{-9}	77	5.4	--
Oed. #177	Oct. 27/71	15	0.306	6.82×10^{-8}	50	1.0	--
Oed. #179	Oct. 30/71	15	0.306	8.23×10^{-9}	76	6.6	-- *
Oed. #177	Oct. 30/71	15	0.306	1.19×10^{-7}	51	0.55	--
Oed. #179	Nov. 17/71	15	0.306	7.16×10^{-9}	76	3.0	--
Triaxial #2	Nov. 19/71	15	0.306	8.44×10^{-9}	56.2	13.9	--
Oed. #177	Dec. 1/71	5	0.622	1.30×10^{-7}	80	0.80	-- *
Oed. #179	Dec. 17/71	15	0.622	7.02×10^{-9}	76	12.5	--
Oed. #177	Jan. 5/72	5	0.622	1.02×10^{-7}	76	0.12	-- *
Oed. #177	Jan. 7/72	5	0.622	1.25×10^{-7}	50	1.35	--
Oed. #179	Jan. 24/72 (15:34)	15	0.622	7.02×10^{-9}	50	32.5	0.77
Oed. #179	Jan. 24/72 (16:19)	15	0.622	7.02×10^{-9}	50	11.8	0.10
Triaxial #2	Feb. 18/72 (10:55)	5	0.622	1.03×10^{-7}	52	1.41	0.15
Triaxial #2	Feb. 18/72 (11:03)	5	0.622	1.03×10^{-7}	52	1.33	0.10
Oed. #177	Feb. 18/72 (9:15)	5	0.622	8.36×10^{-8}	50	3.9	0.19
Oed. #177	Feb. 18/72 (9:28)	5	0.622	8.36×10^{-8}	50	2.75	0.16
Oed. #177	Feb. 22/72 (9:15)	5	0.622	1.13×10^{-7}	50	1.40	0.11
Oed. #177	Feb. 22/72 (9:42)	5	0.622	1.13×10^{-7}	70	0.73	0.02
Oed. #177	Feb. 22/72 (10:44)	5	0.622	1.13×10^{-7}	30	1.5	0.03
Oed. #177	Feb. 22/72 (11:17)	5	0.622	1.13×10^{-7}	50	--	--
Oed. #177	Feb. 22/72 (13:10)	5	0.622	1.16×10^{-7}	50	0.46	0.13
Oed. #177	Feb. 22/72 (13:19)	5	0.622	1.16×10^{-7}	50	0.42	0.01
Oed. #177	Feb. 22/72 (13:35)	5	0.622	1.16×10^{-7}	50	4.60	4.20

*Disc was cracked

the characteristic shape predicted by the theory. The upper portion, approaching 100 percent response, is slightly slower in reaching 100 percent than the theory predicts. The pore pressure response curves could be essentially reproduced with only a slight horizontal translation due to differing air contents (Figure 10). If the amount of air entrapped in the compartment was modified between two consecutive tests, the response curves shifted laterally (Figure 11). The volume of entrapped air was measured using a diffused air volume indicator (Fredlund, 1973).

The compressibility plots (Figures 9 and 12) have the same shape as the theoretical curves up to a response of approximately 80 percent. At this point the curves tend to the right, indicating an increase in compressibility. Several factors may be involved in this phenomenon. With the increasing elapsed time, some air may be dissolved in the water. Assuming a one-dimensional diffusion model with air overlying water, an estimate was made of the significance of diffusion (Figure 13). Although diffusion shows the correct trend, it does not appear to completely account for the observed behavior. Minute volume changes associated with the seating of the components of the compartment (e.g., O-rings in the valves) may be significant during the final stages of equalization.

COMPARISON OF EXPERIMENTAL DATA WITH THE THEORY

The theoretical analysis showed that only two variables were required to define the response curves (i.e., slope of the response

curve and the equalization time). Since the slope of the response curve is dependent on only the applied pressure, there is a unique relationship between the slope of the response curve and the applied chamber pressure (Figure 14). The experimental results all lie close to the theoretical line, indicating good agreement. The moderate scatter is partly related to the difficulty in accurately measuring the slope of the response curve. However, other factors are likely involved as well.

The experimental and theoretical times for equalization (for an applied pressure of 50 psi) are compared on Figure 15. The equalization time is assumed fixed and can be plotted versus the measurement of either the initial amount of air or the compliance factor. The percent air is estimated either by flushing the compartment and measuring the volume of air or from the computed compressibility versus pressure plot. The results indicate close agreement between the compliance factor and the percent air computed from the data. In three cases, the measured air content is too low. This indicates that all the air was not removed during the flushing process. Probably higher flushing pressures would have proven more successful.

There is also the possibility that there was not as much air in the compartment as the theoretical computations show. However, if this is the case, the compressibility due to the volume change of the compartment must also be non-linear and behave as an air-water mixture. In other words, either interpretation verifies the assumed constitutive relationship.

The experimental data shows reasonable agreement with the

theory for both the slope of the response curve and the equalization time. This lends credence to the assumed constitutive relationship for the air-water mixture. The effect of air and the difficulty of obtaining a completely saturated measuring system are clearly depicted. An assumption that the compressibility of the fluid in the measuring system is equal to that of pure water could not produce results similar to those presented.

REFERENCES

Christie, R.F. (1965) *"Secondary Compression Effects During One-Dimensional Consolidation Tests"*, Proc. Sixth International Conference on Soil Mech. and Fdtn. Eng., Montreal, Vol. 1, pp 198-202.

Fredlund, D.G. (1973) *"Volume Change Behavior of Unsaturated Soils"*, Ph.D. thesis, University of Alberta.

Gibson, R.E. (1963) *"An Analysis of System Flexibility and Its Effects on Time - Lag in Pore-Water Pressure Measurements"*, Geotechnique, Vol. 13, pp 1-11.

Northey, D. and F. Thomas (1965) *"Consolidation Test Pore Pressures"*, Proc. Sixth Int. Conf. on Soil Mech. and Fdtn. Eng., Montreal, Vol. 1, pp 323-327.

Perloff, W.H., K. Nair and J.G. Smith (1965) *"Effect of Measuring System on Pore Water Pressures in the Consolidation Test"*, Proc. Sixth Int. Conf. on Soil Mech. and Fdtn. Eng., Montreal, Vol. 1, pp 338-341.

Whitman, R.V., A.M. Richardson and K.A. Healy (1961) *"Time-lags in Pore Pressure Measurements"*, Proc. Fifth International Conference on Soil Mechanics and Foundation Engineering, Vol. 1, pp 407-411.

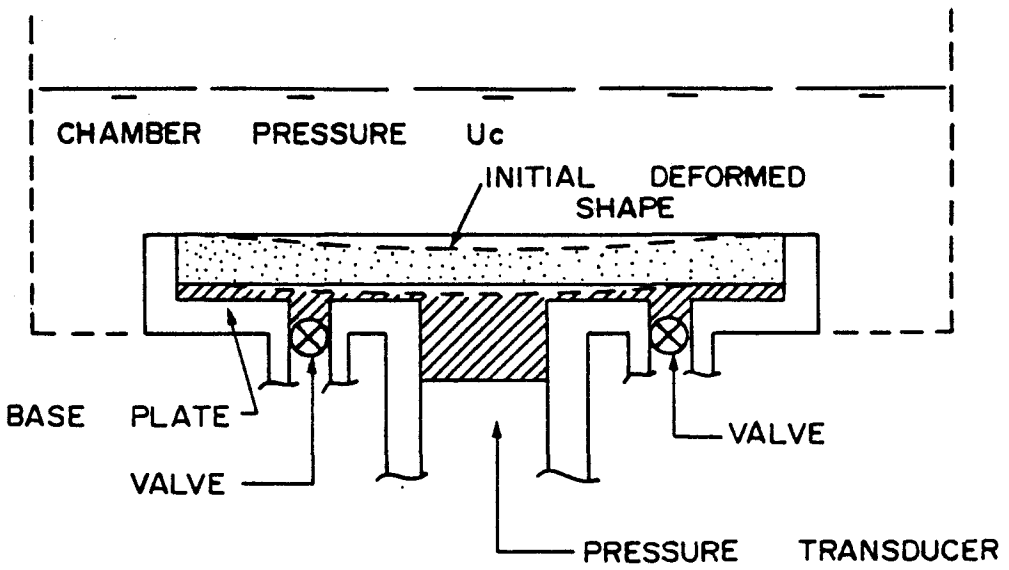

(a) INSTANT AFTER CLOSING VALVES AT THE END OF STEADY STATE SEEPAGE

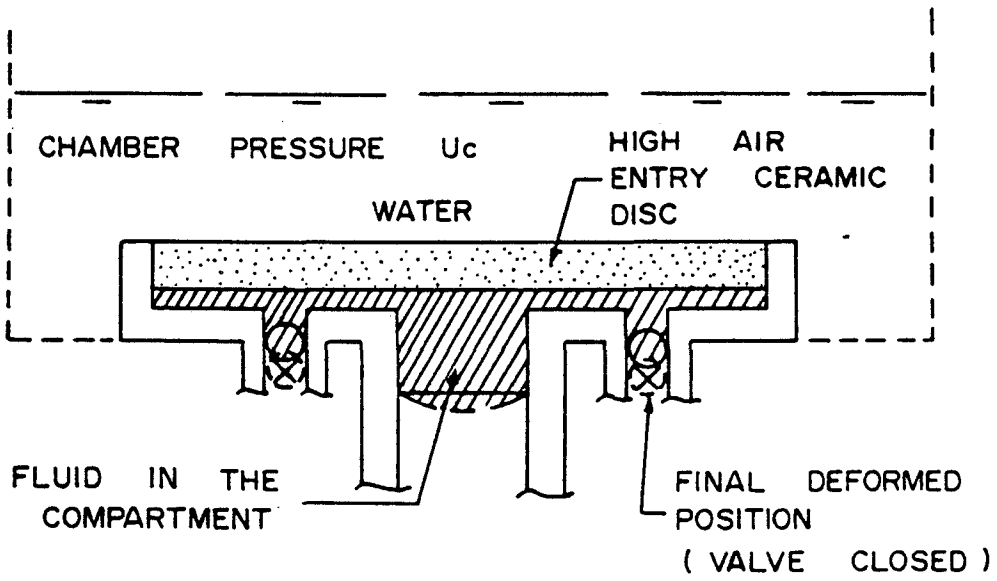

(b) AT EQUILIBRIUM

FIGURE 1 CHARACTERIZATION OF THE PRESSURE MEASURING SYSTEM

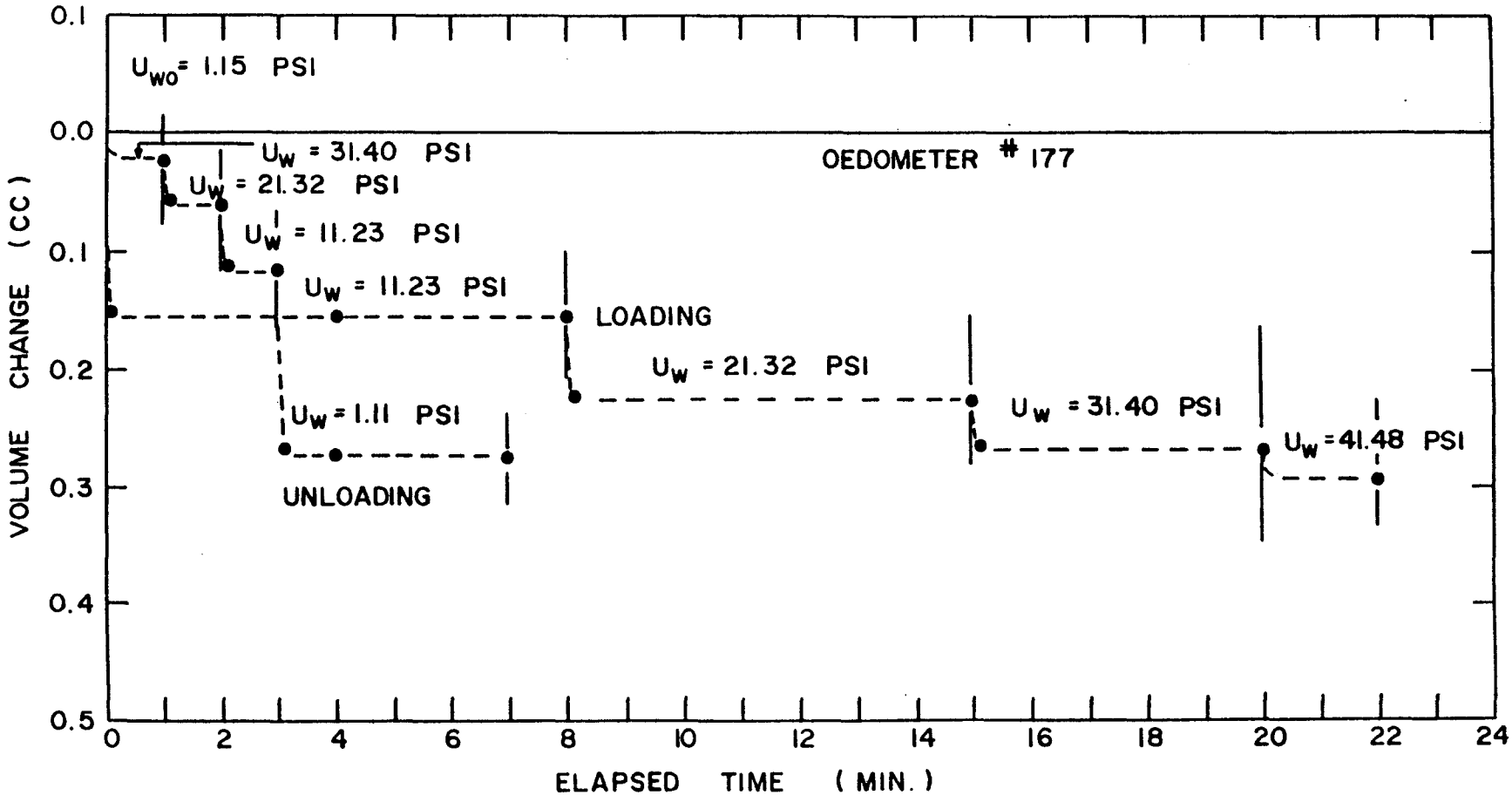

FIGURE 2 VOLUME CHANGE IN THE COMPARTMENT OF OEDOMETER NO. 177 DURING LOADING AND UNLOADING

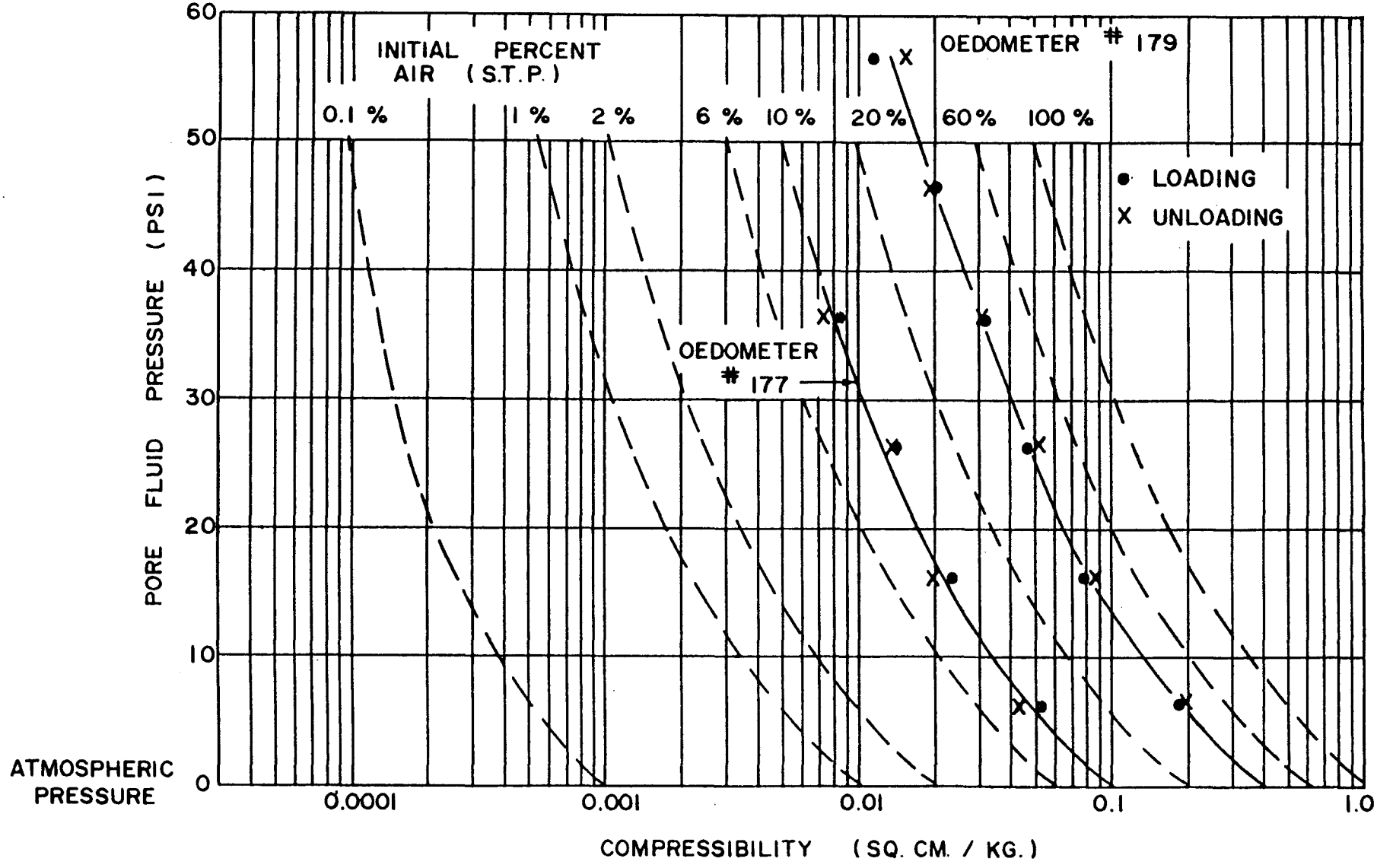

FIGURE 3 MEASURED COMPRESSIBILITIES IN THE COMPARTMENT OF OEDOMETERS NO. 177 AND NO. 179

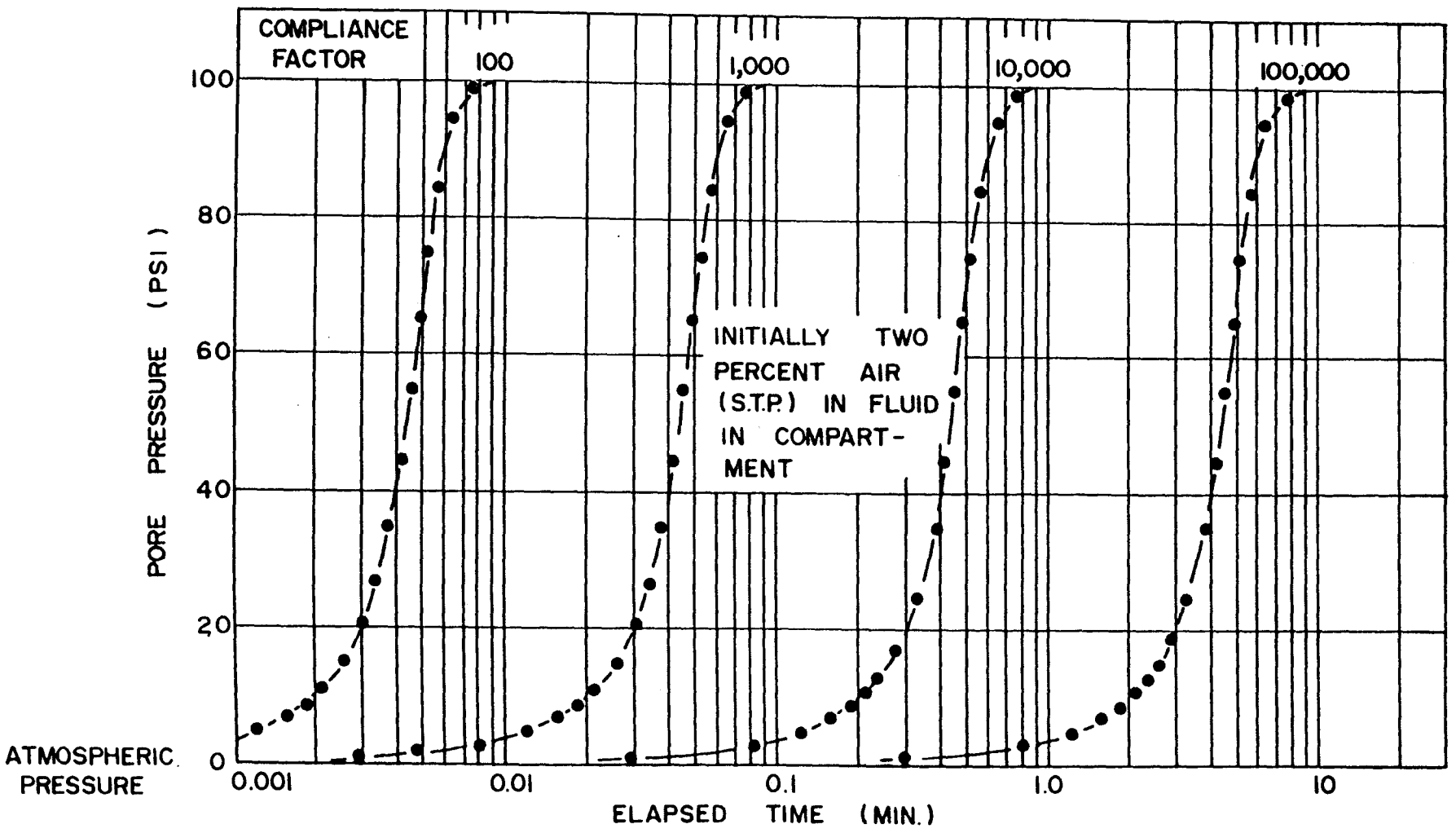

FIGURE 4 PORE PRESSURE RESPONSE CURVES FOR VARIOUS COMPLIANCE FACTORS (TWO PERCENT AIR S.T.P.)

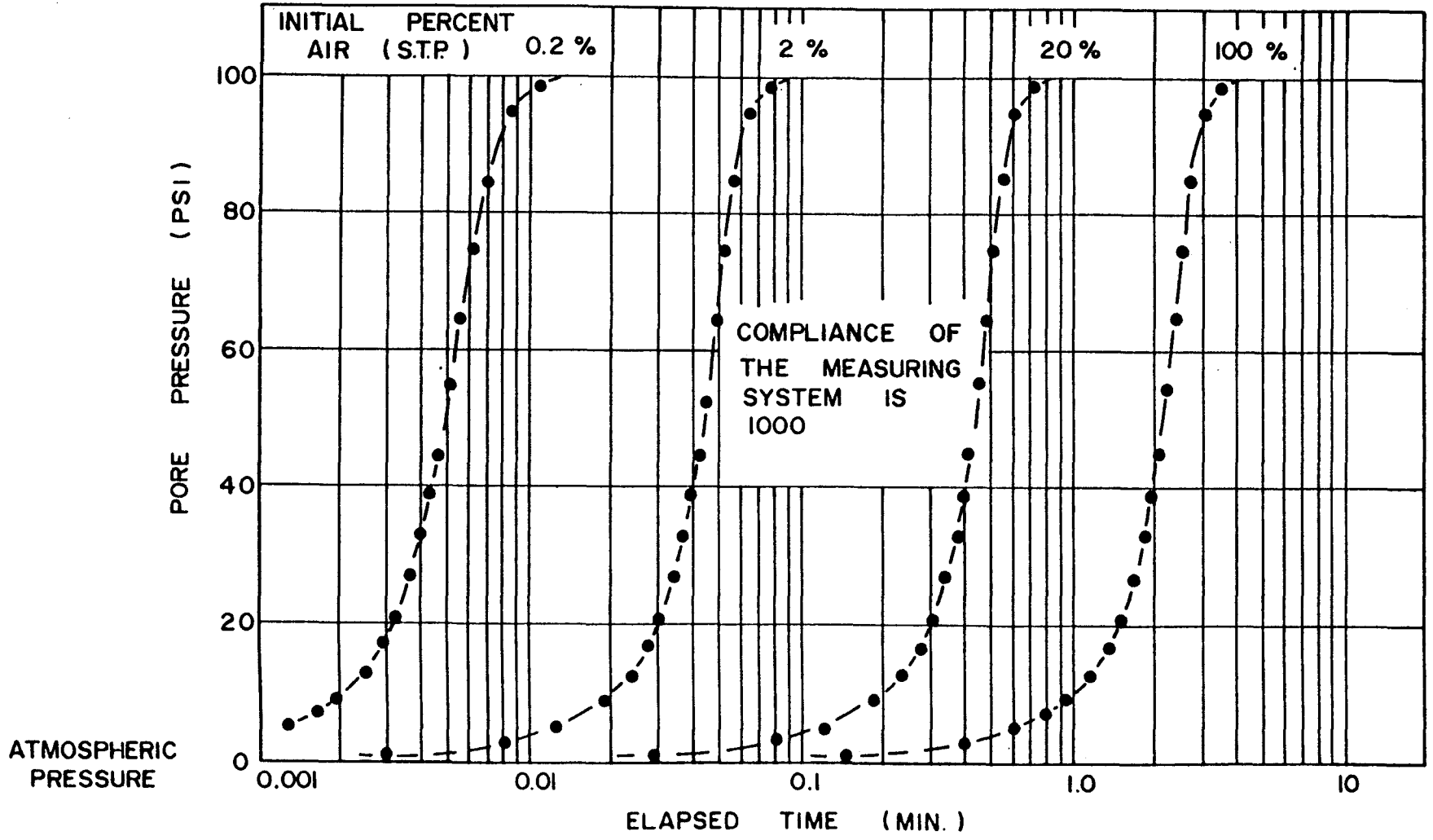

FIGURE 5 PORE PRESSURE RESPONSE CURVES FOR VARIOUS PERCENTAGES OF AIR IN THE COMPARTMENT (COMPLIANCE = 1000)

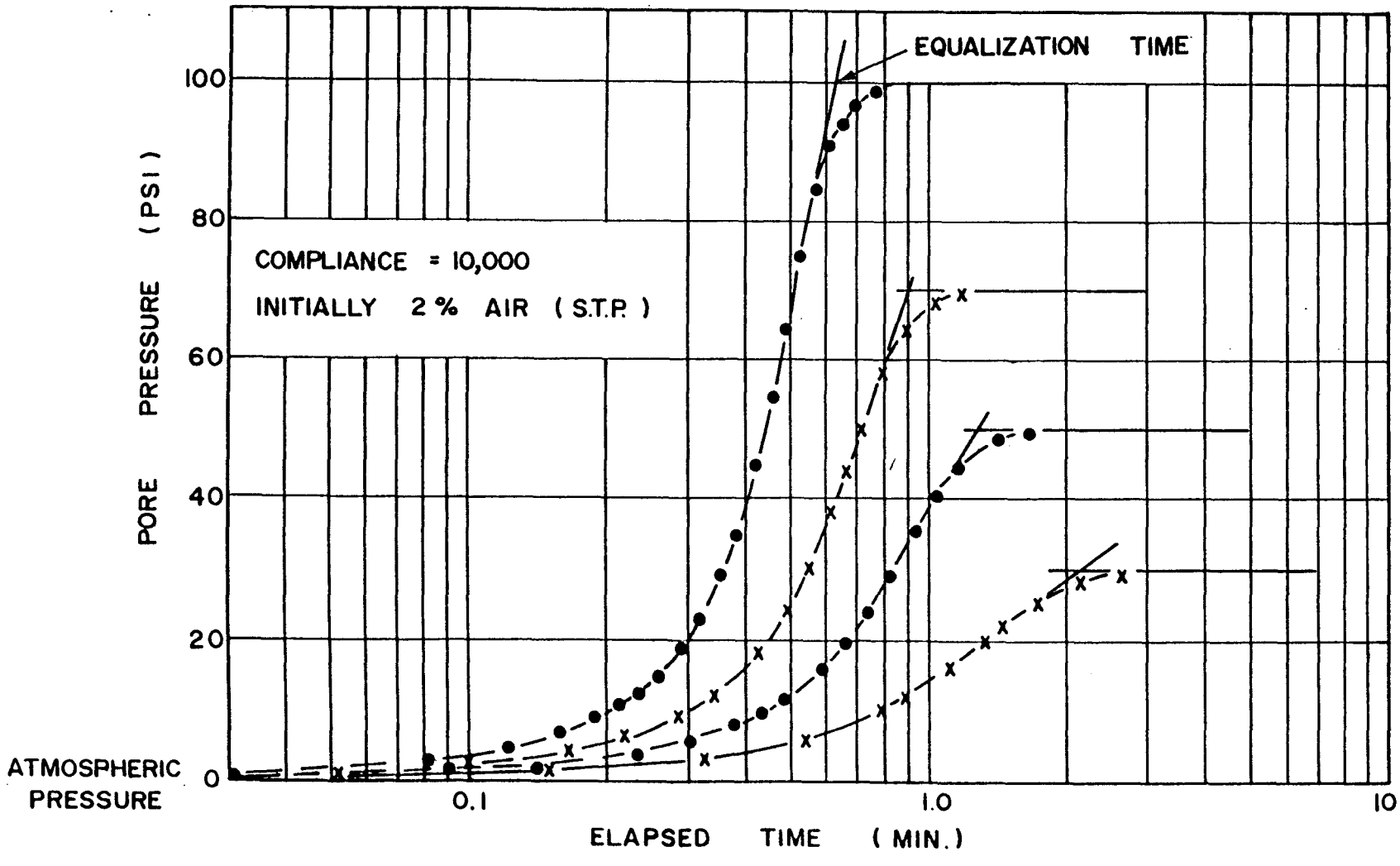

FIGURE 6 PORE PRESSURE RESPONSE CURVES FOR VARIOUS APPLIED PRESSURES

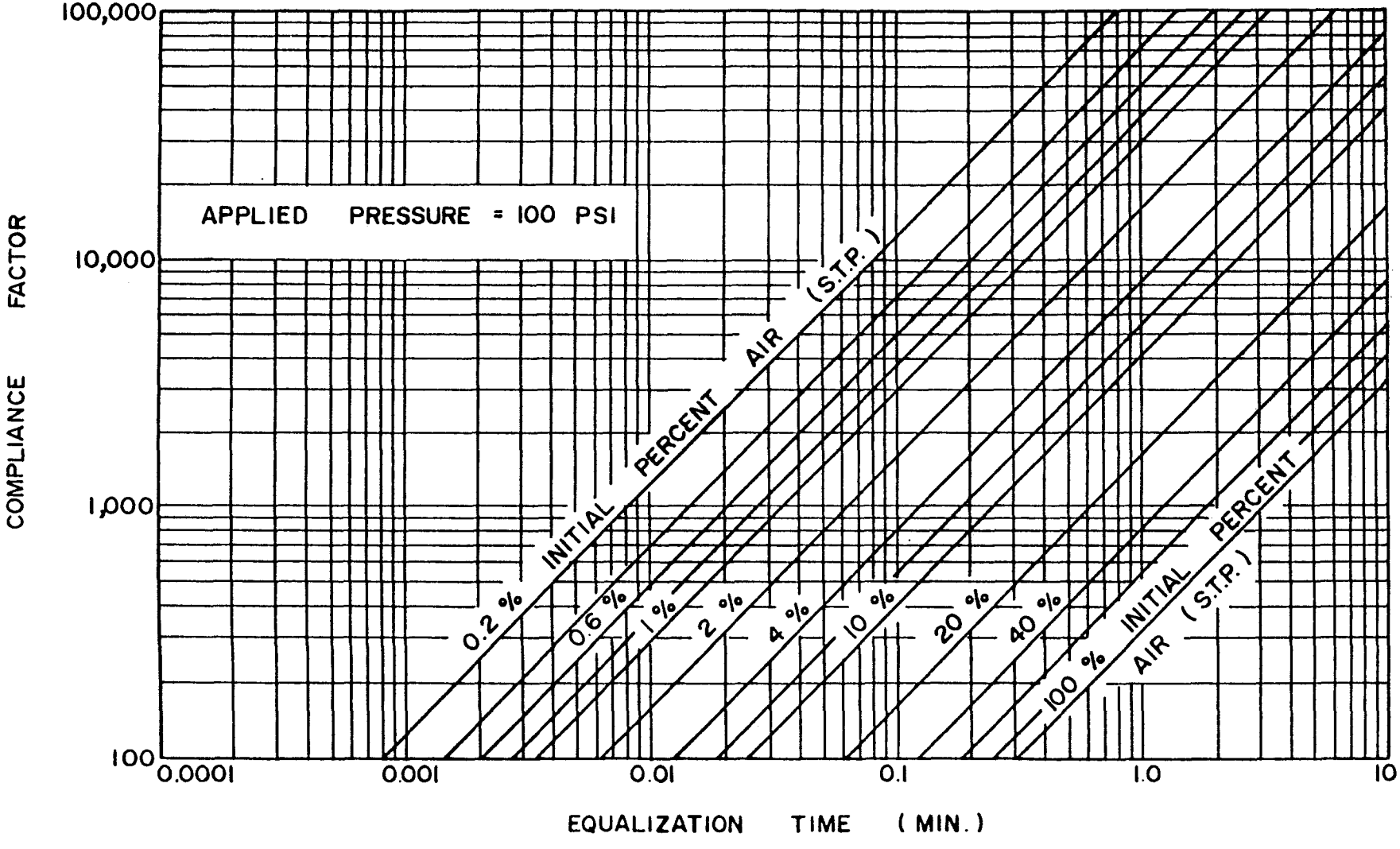

FIGURE 7 TIME FOR PORE PRESSURE EQUALIZATION FOR AN APPLIED PRESSURE OF 100 PSI

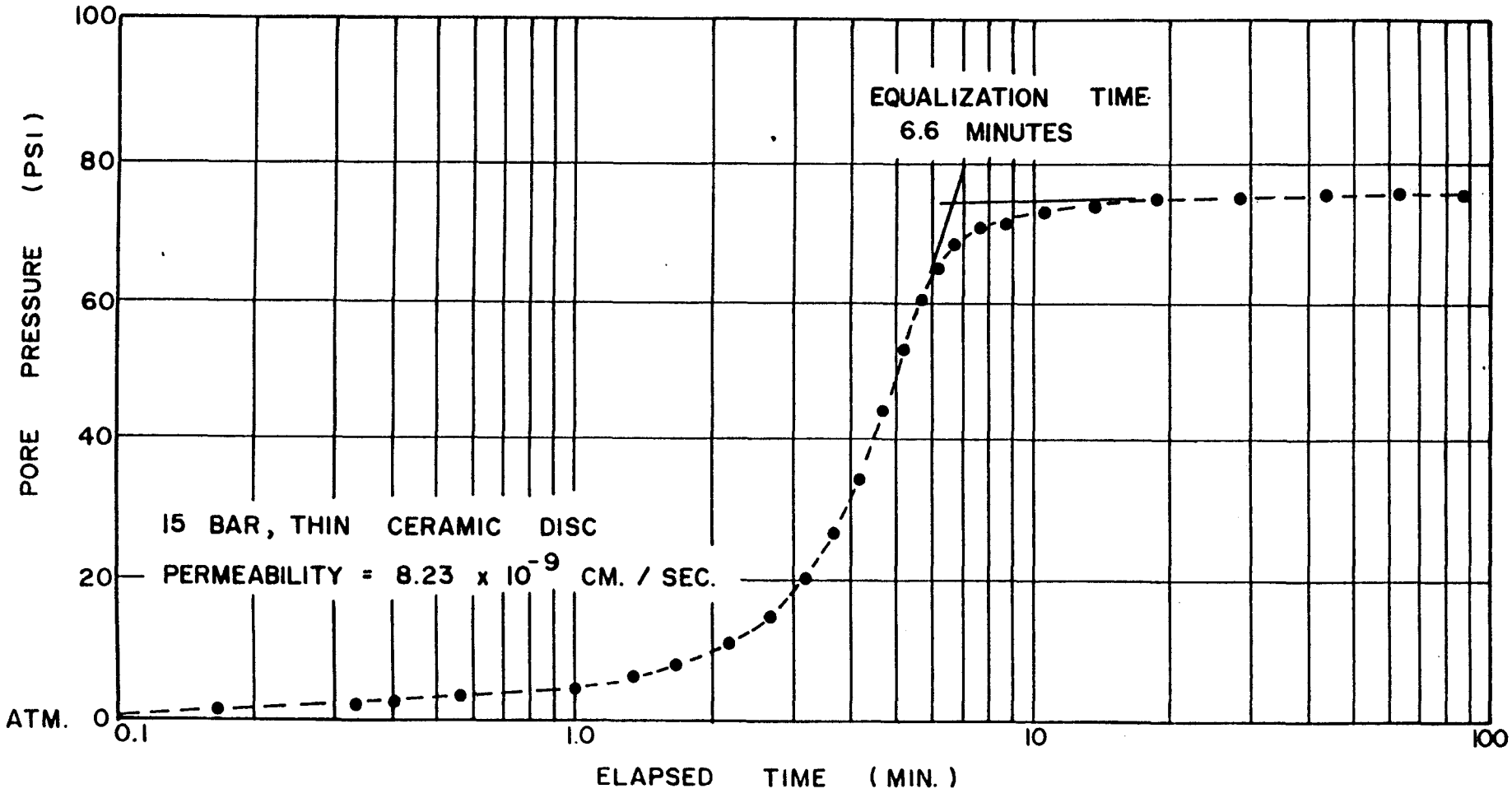

FIGURE 8 PRESSURE RESPONSE ON ANTEUS OEDOMETER # 179

(OCT. 30, 1971)

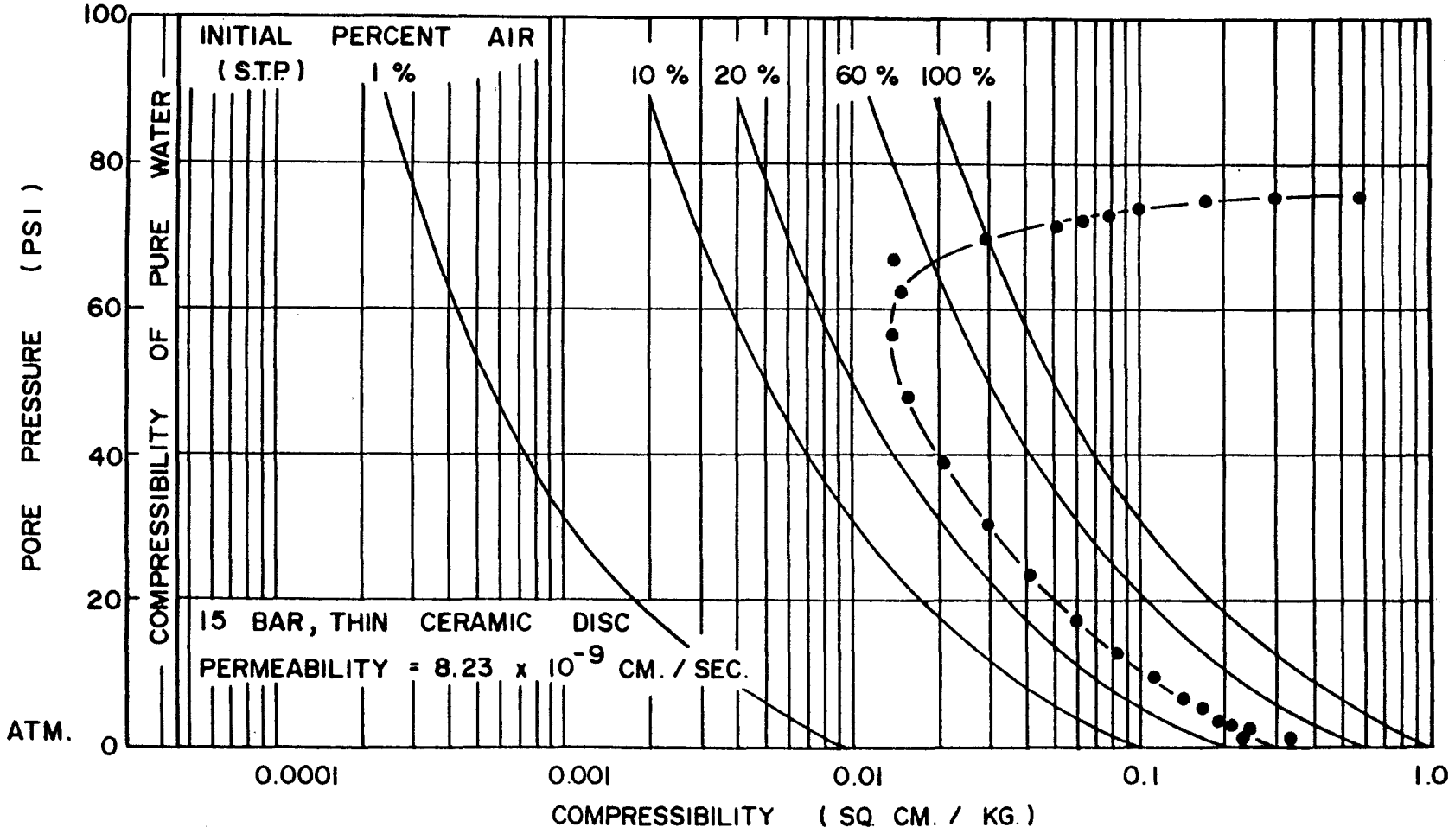

FIGURE 9 COMPRESSIBILITY OF THE FLUID IN THE PORE PRESSURE MEASURING SYSTEM ON ANTEUS OEDOMETER # 179
(DECEMBER 30, 1971)

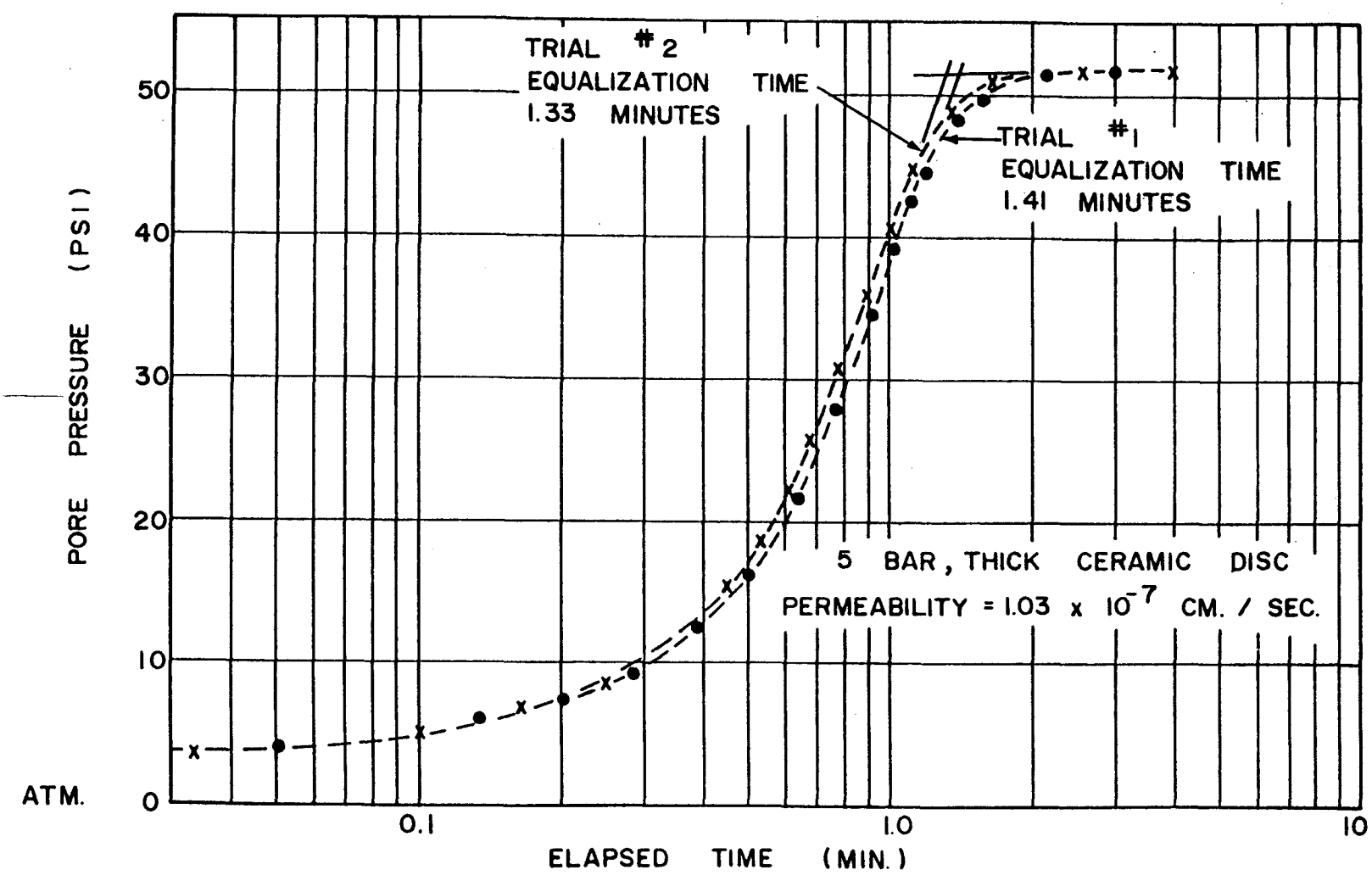

FIGURE 10 PRESSURE RESPONSE FOR TRIAXIAL # 2
(FEB. 18, 1972)

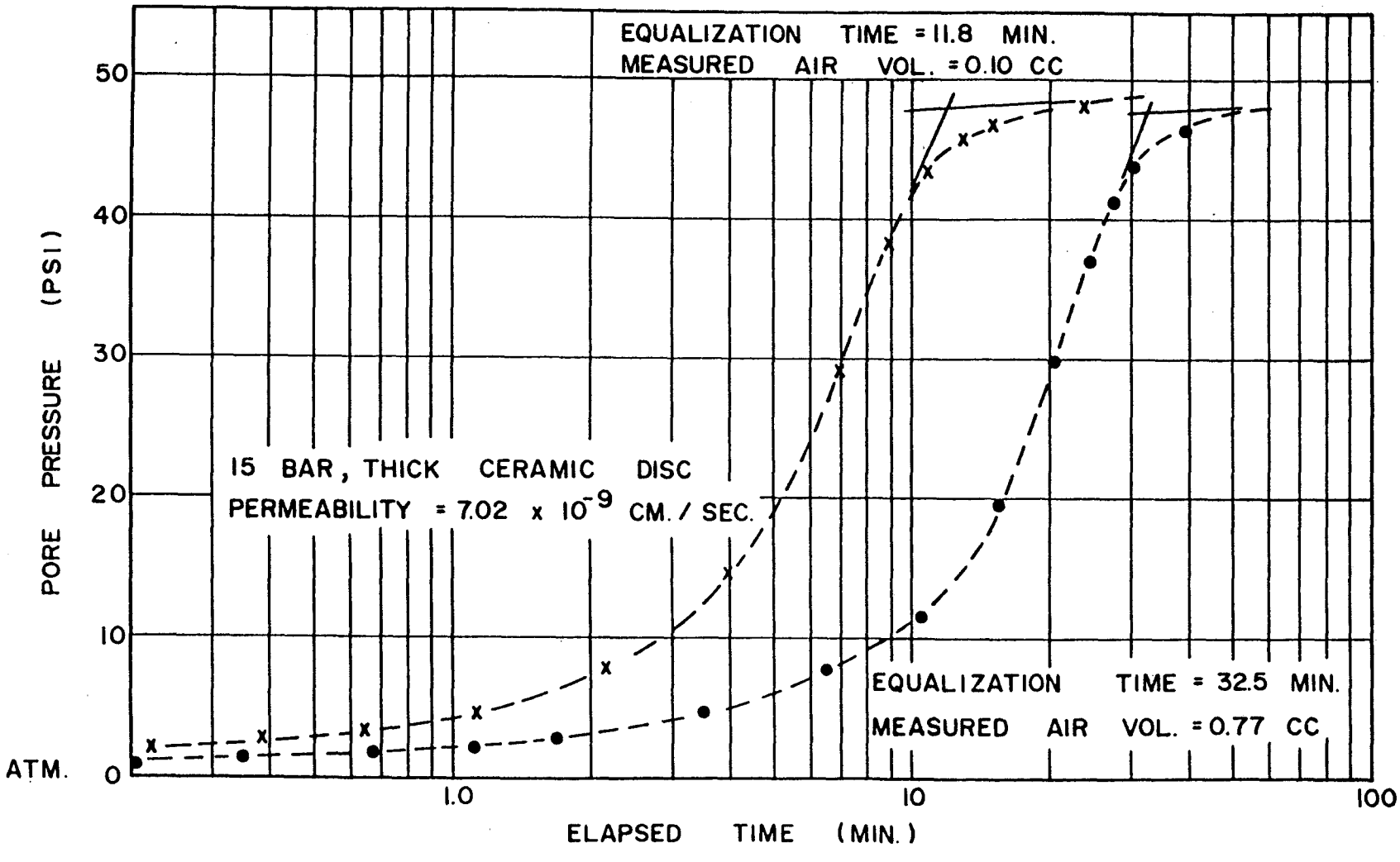

FIGURE 11 PRESSURE RESPONSE ON OEDOMETER # 179
(JAN. 24, 1972)

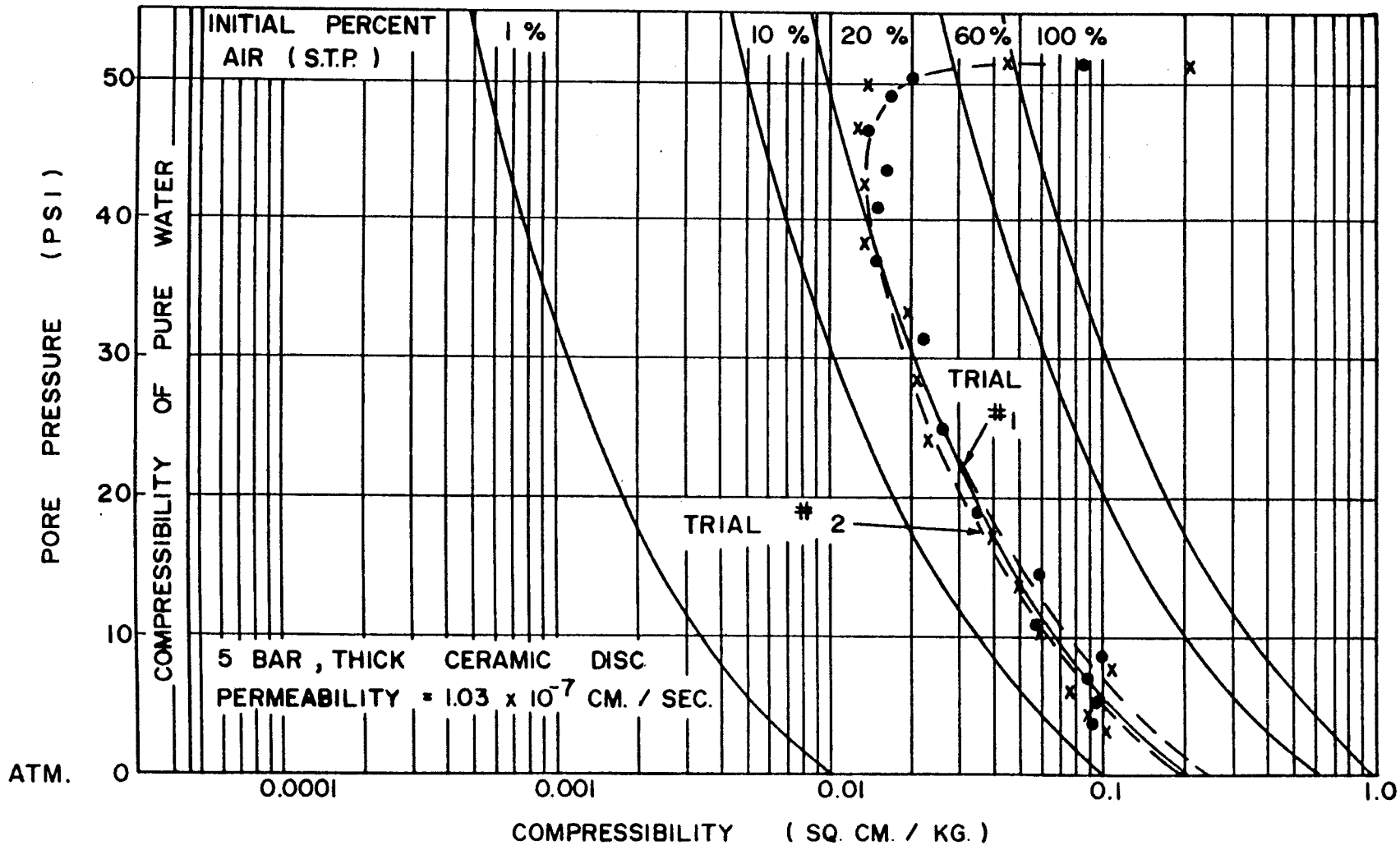

FIGURE 12 COMPRESSIBILITY OF THE FLUID IN THE PORE PRESSURE MEASURING SYSTEM ON TRIAXIAL # 2 (FEB. 18, 1972)

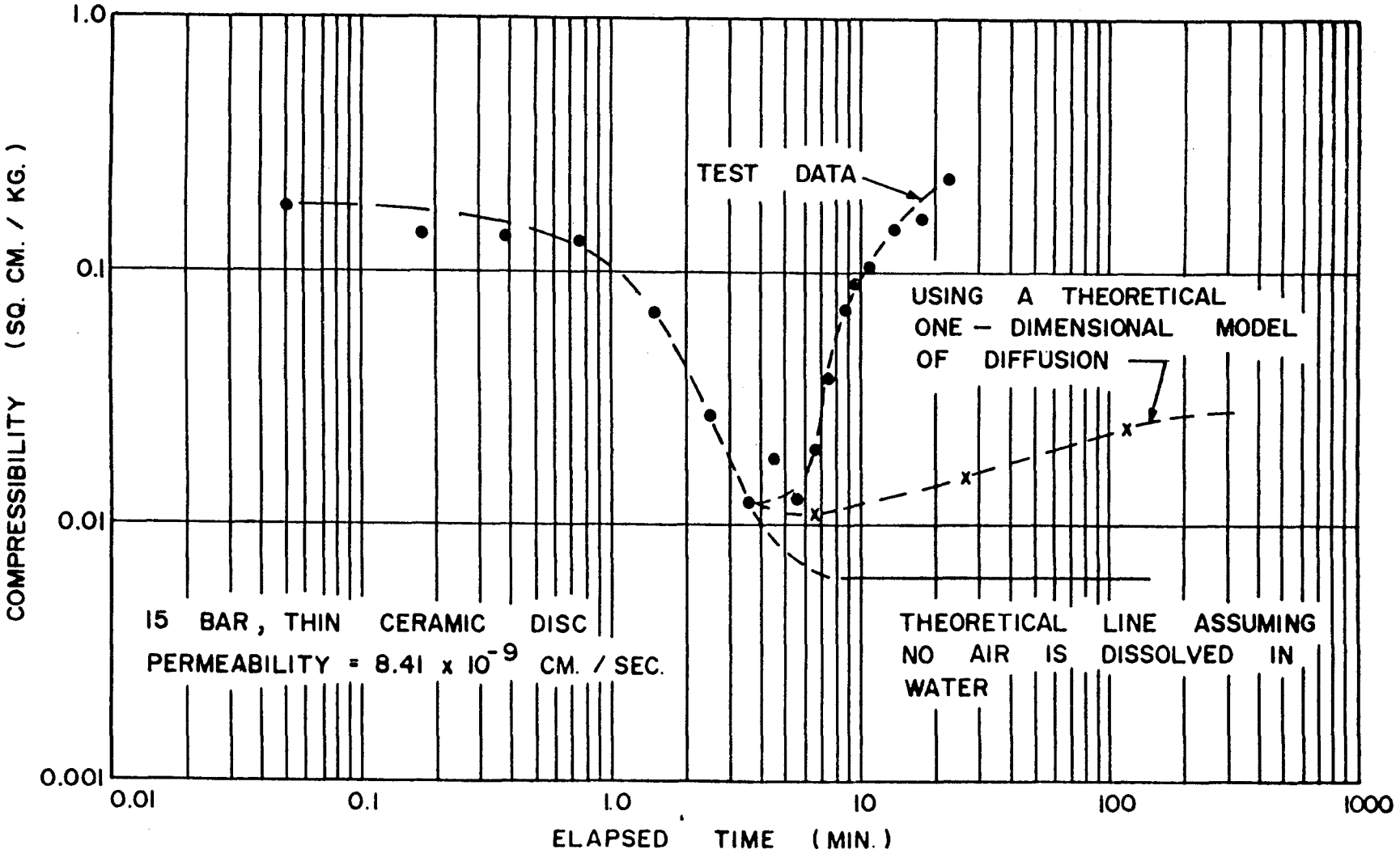

FIGURE 13 DEVELOPMENT OF COMPRESSIBILITY WITH TIME FOR OEDOMETER # 179 (OCT. 27, 1971)

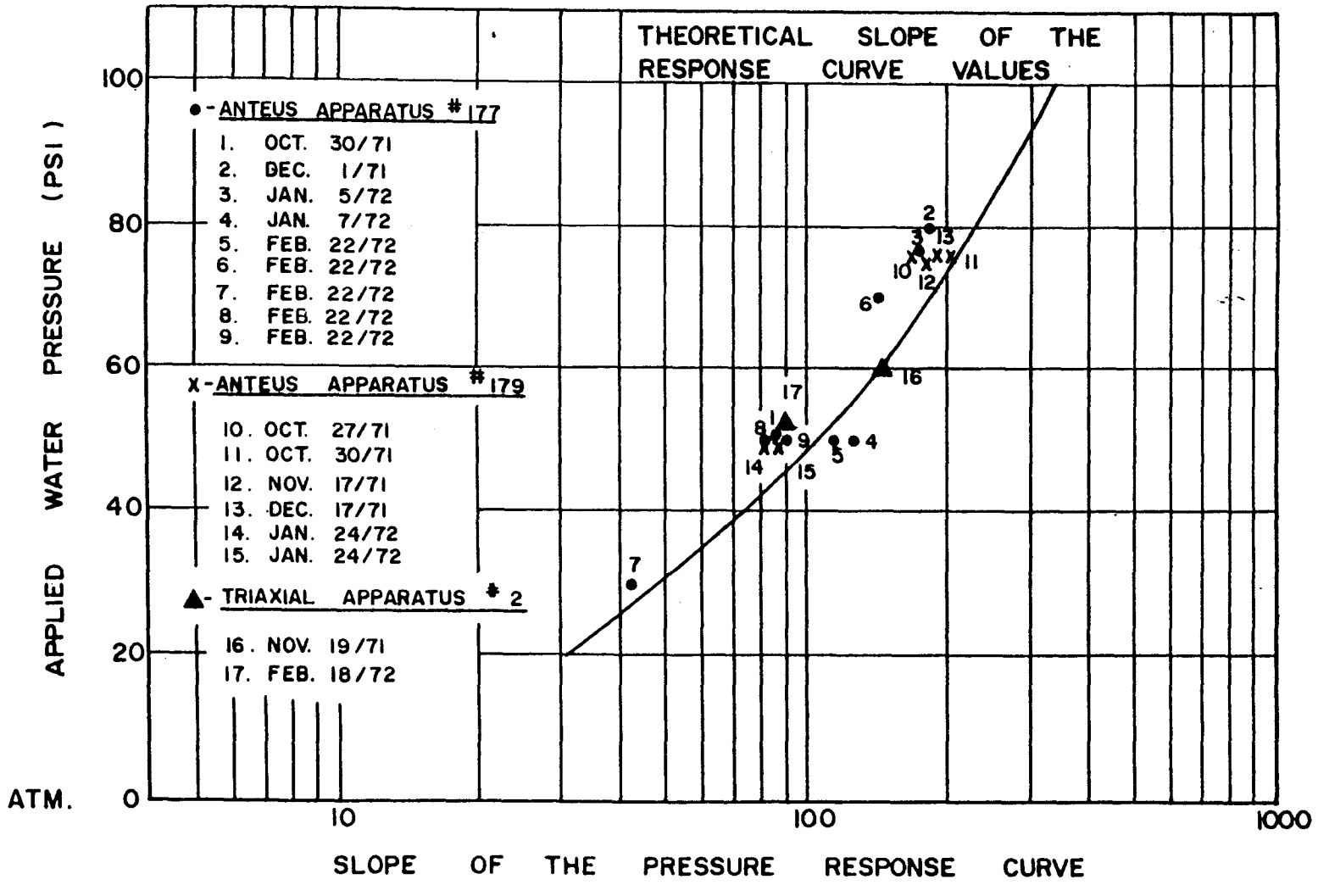

FIGURE 14 COMPARISON OF THE EXPERIMENTAL 'SLOPE OF THE RESPONSE CURVE' WITH THEORETICAL VALUES

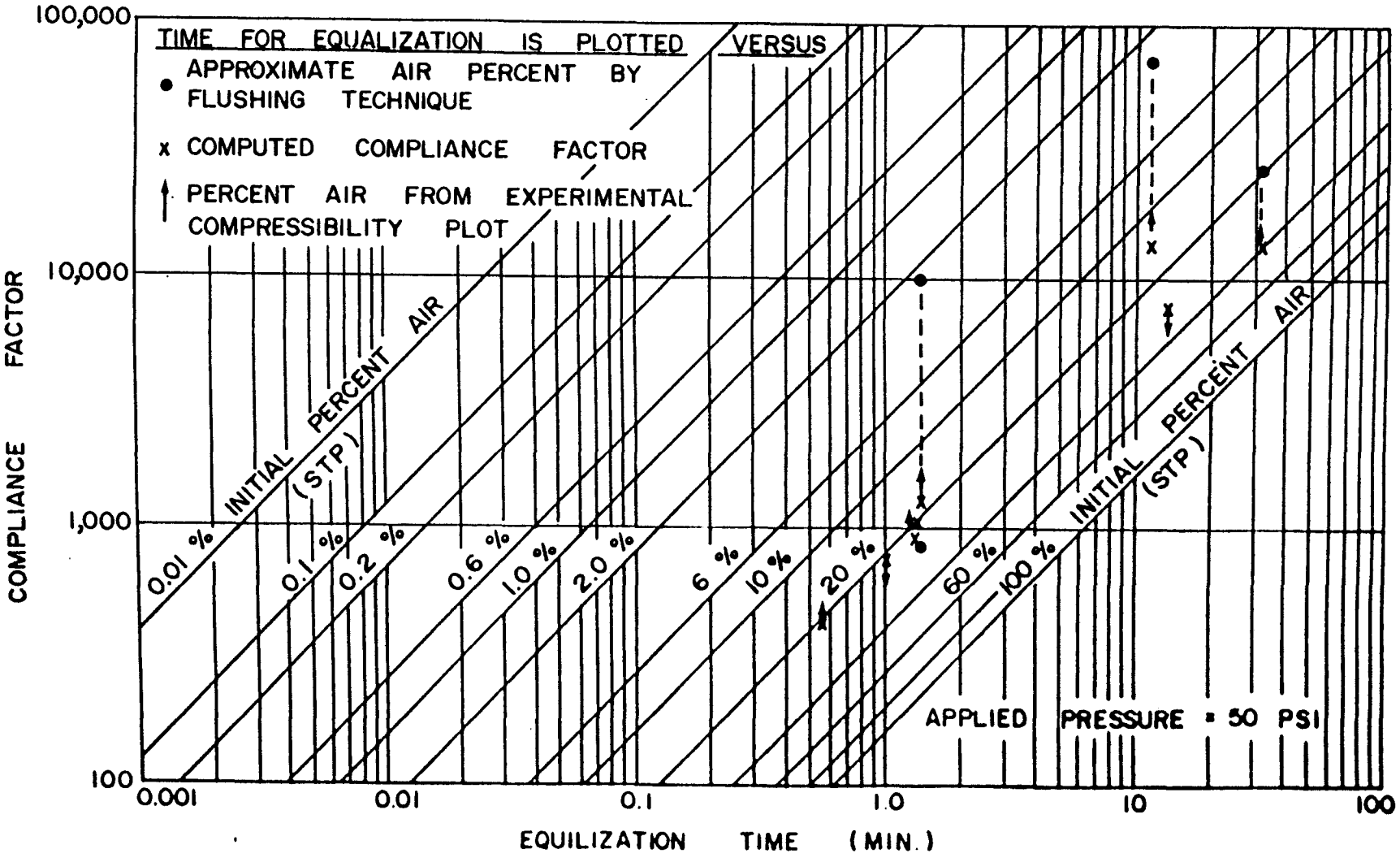

FIGURE 15 COMPARISON OF EXPERIMENTAL AND THEORETICAL TIMES FOR PRESSURE EQUALIZATION

LIST OF RESEARCH PAPERS

	Report No.
Geotechnical Analysis of Pleistocene Deposits in Southern Saskatchewan by E.K. Sauer, Presented to the 26th Annual Canadian Geotechnical Conference, Toronto, October, 1973.	RP – 1
On Total, Matric and Osmotic Suction by J. Krahn and W.G. Fredlund, Soil Science Journal, Volume 114, No. 5, November, 1972.	RP – 2
Some Fatigue Considerations in the Design of Asphalt Concrete Pavements by A.T. Bergan and R.W. Culley, Symposium on Frost Action Roads, Report II, Oslo, Norway, October, 1973.	RP – 3
Characterization of Freeze-Thaw Effects on Subgrade Soils by A.T. Bergan and D.G. Fredlund, Symposium on Frost Action Roads, Report II, Oslo, Norway, October, 1973.	RP – 4
Pressure Response Below High Air Entry Discs by D.G. Fredlund and N.R. Morgenstern, Third International Research and Engineering Conference on Expansive Soils, Haifa, Israel, August, 1973.	RP – 5
Moving Grain in the 70's by Gordon A. Sparks, Annual Conference of the Roads and Transportation Association of Canada, Halifax, Canada, October, 1973.	RP – 6
Optimal Spacing of Country Elevators in Western Canada by Gordon A. Sparks, Annual Conference of the Transportation Research Forum, Cleveland, U.S.A., October, 1973.	RP – 7